MANUFACTURING AND CHARACTERIZATION OF RF-MEMS SWITCHES BUILT ON ALUMINA BY USING STANDARD MULTILAYER THIN FILM EQUIPMENT

S. Di Nardo[(1)], E. Di Paola[(1)], P. Farinelli[(2)], G. Mannocchi[(3)], U. Di Marcantonio[(1)], R. Sorrentino[(2)]

[(1)]Alcatel Alenia Space
Via Pile 60, 67100 L'Aquila, Italy
Email: sergio.dinardo@aleniaspazio.it

[(2)] DIEI - Università di Perugia
Via G. Duranti 93, 06125 Perugia, Italy
Email: farinelli@diei.unipg.it

[(3)]Alcatel Alenia Space
Via Saccomuro 24, 00131, Roma, Italy

INTRODUCTION

In recent years increasing attention has been devoted to microelectromechanical systems (MEMS) for a number of electronic applications. In this paper we focus our attention to microelectromechanical switches. Originally proposed by Petersen in 1979 [11] MEMS technology is presently on the verge of revolutionizing RF and microwaves applications.
The increasing market demand for more functional devices has generated the need of a more flexible and easy realization process, where low cost, weight and size are the most important requirements.
The realization of electrostatics switches on alumina substrates is demonstrated in this work. The theoretical characterization based on the electrostatic 1D model is compared with experimental data.

MEM SWITCH PROCESS FLOW

We explain here the realization process for a shunt switch with ohmic contact. Figure 1 shows the main steps for the switch manufacturing. We can summarize this flow in six steps:

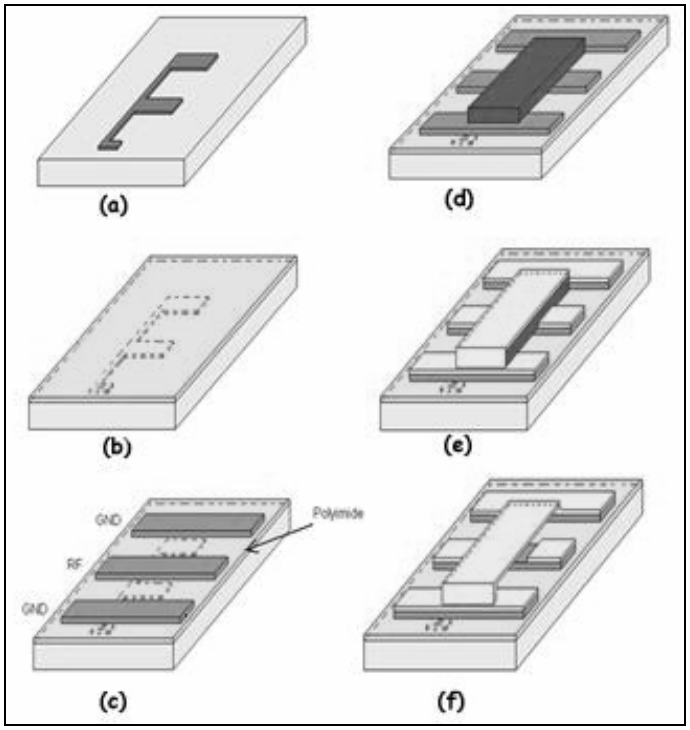

Fig. 1. Switch shunt process flow

a) A NiCr+O_2 film 200 Å thick is grown onto an alumina substrate by sputtering process, so that bias lines can be defined. This film has a sheet resistivity ~1300 Ω/sq.
b) The bias lines are covered by a dielectric layer of polyimide (thickness 2,5 μm, ε_r=2,9).
c) On this dielectric layer a NiCr-Au film is grown (0,5 μm) for the coplanar waveguide (CPW) photolithography. In such a way the actuation pads lye at the edges of the RF line.
d) A 2,5μm photoresist sacrificial layer is deposited.
e) The gold structural layer is deposited by a first sputtering process (0,5 μm) and a second electroplating growth. The total thickness of the multilayer is 2 μm.
f) Finally, the sacrificial layer is removed by wet etching (acetone).

ANALYTICAL MODEL

In order to predict the electro-mechanical behaviour of the micro-switches, the conventional analytical model has been applied. This model is based upon a simple representation [1] of the real device, as shown in figure 2.

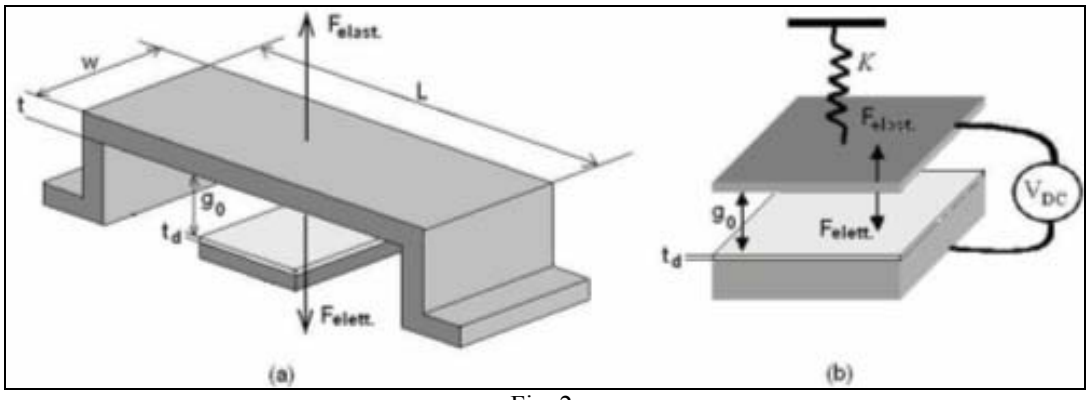

Fig. 2.

The model consists of two parallel conducting plates forming a capacitor where the upper plate is held by a spring, characterized by its effective stiffness K_{eff} .
The capacitance between the two metal plate is given by:

$$C = \frac{\varepsilon_0 A}{g_0 + \frac{t_d}{\varepsilon_r}} \tag{1}$$

where A is the overlap area between the bridge and the actuation pads, g_0 the air gap, ε_r and t_d the dielectric constant and thickness of the dielectric layer covering the pads. Note that equation (1) does not account for fringing field effects and charge redistributions [2]-[4]. When an appropriate DC voltage is applied an electro-mechanical instability occurs, the movable plate collapses and the device is actuated. The pull-in voltage is given by:

$$V_{PI} = \sqrt{\frac{8K_{eff}}{27\varepsilon_0 A}\left(g_0 + \frac{t_d}{\varepsilon_r}\right)^3} \tag{2}$$

If the voltage is reduced below the so called hold-down voltage V_{HD}, the electrostatic force is smaller than the elastic restoring force so the bridge is pulled-out:

$$V_{HD} = \sqrt{\frac{2K_{eff}\, g_0 t_d^2}{\varepsilon_0 \varepsilon_r{}^2 A}} \tag{3}$$

The computation of (2) and (3) requires the knowledge of $K_{eff.}$
Nevertheless, it is possible to extrapolate some structural information by measuring the ratio V_{PI}/V_{HD} since this ratio is only function of the geometrical parameters g_0 and t_d besides the electrical parameter ε_r.
Let us consider the air gap g_0 (nominally 2,5μm). Figure 3 shows the ratio V_{PI}/V_{HD} as a function of g_0 for t_d=2,5μm and ε_r=2,9.

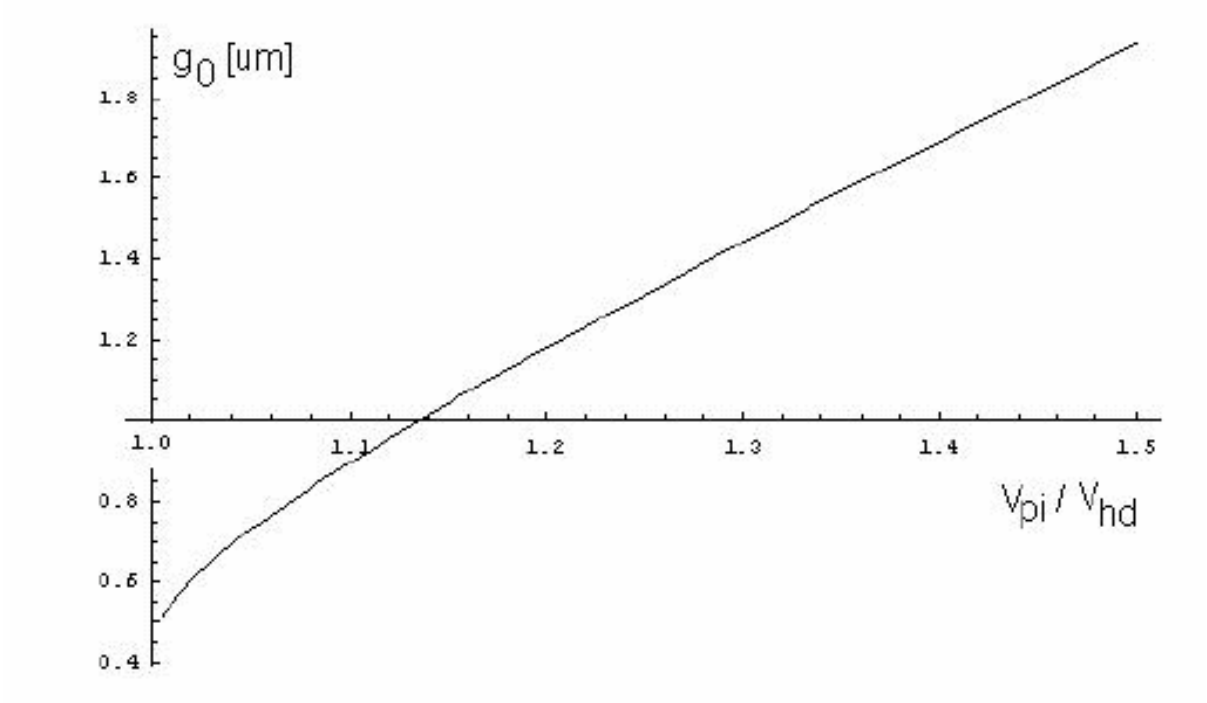

Fig. 3.

In figure 4 we can see the numerical values of V_{PI} and V_{HD} for five structures, together with the values of g_0 found from the ratio V_{PI}/V_{HD}: it is evident that in all the structures the gap is lower than the nominal value 2,5μm and consequently this leads to an higher Up State Capacitance of the bridge that should be taken into account in the design phase.

$St.$	V_{pi}^0	V_{hd}^0	g_0 $[\mu m]$
1	29 ± 3	26 ± 3	$0,94 \pm 0,05$
2	33 ± 3	28 ± 3	$1,12 \pm 0,05$
3	30 ± 3	26 ± 3	$1,05 \pm 0,05$
4	32 ± 3	28 ± 3	$1,03 \pm 0,05$
5	42 ± 3	35 ± 3	$1,18 \pm 0,05$

Fig. 4.

MODELLING THE EFFECTIVE STIFFNESS CONSTANT K_{eff}

In this section we will derive an analytical expression for K_{eff} starting from the calculation of the beam's bending for a constant load (no electrostatic force). This bending (like K_{eff}) is related to the geometrical configuration of the switches (width w, thickness h, pad positions) as well as to its structural parameters (Young modulus E, Poisson ratio ν) (see figure 5).

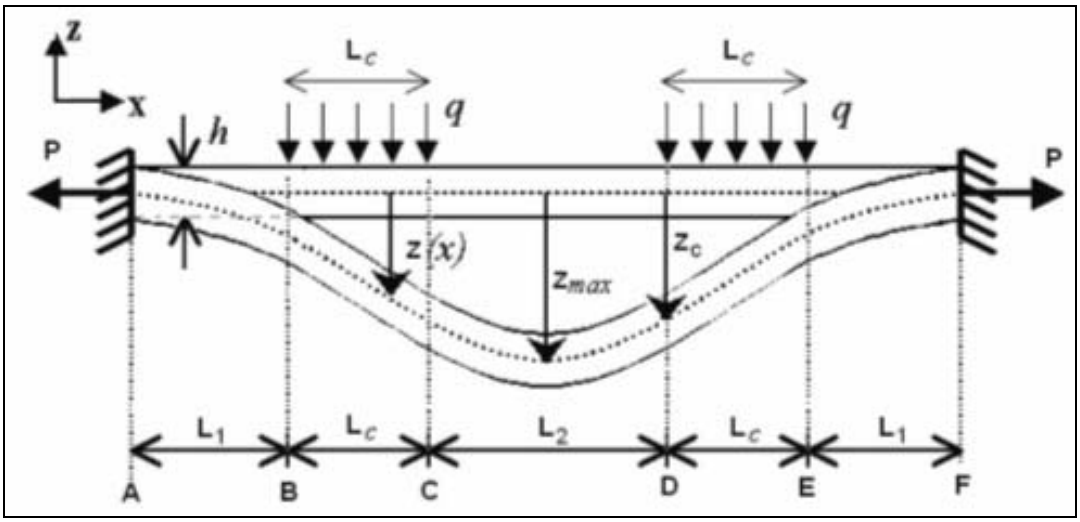

Fig. 5.

In order to find the bending we can write the following equation for z(x) [5] [6]:

$$\frac{d^2 z(x)}{dx^2} = \frac{M_b(x)}{E' I} \tag{4}$$

where $I=wh^3/12$ is the inertial moment and E' is the *effective* Young modulus for a wide beam [7] (a beam is considered wide when $w \geq 5h$) and its values is: $E'=E/(1-\nu^2)$ (E_{Au}=78,5GPa, ν_{Au}=0,42). M_b is the bending moment and it's related to all forces acting on the beam. The equation (4) must be solved for each stroke A-B, B-C, C-D (we can take advantage of the symmetry too) with the appropriate boundary conditions. The analytical expressions for $M_b(x)$ are:

$$\text{A-B} : M_b(x) = -M_0 + Rx + Pz(x)$$

$$\text{B-C} : M_b(x) = -M_0 + Rx + Pz(x) - (q/2L_C)(x-L_1)^2$$

$$\text{C-D} : M_b(x) = -M_0 + R(L_1 + L_C/2) + Pz(x)$$

Where R is the reaction at the extremity A and M_0 is the reactive moment (R and M_0 represent the interaction with the wall, where the boundary conditions imposed are z=0 and z'=0). The parameter q is the load upon each actuation pad and P is the axial force (unknown). This axial force is related to two main effects:

1) the length variation of the beam which causes an axial stress of the fibres. The correspondent force is:

$$P_1 = hwE'\frac{\Delta L}{L}$$

where

$$\Delta L \approx \int_0^L \left(\frac{dz(x)}{dx}\right)^2 dx$$

and L is the total initial length ($L=2(L_C+L_1)+L_2$).

2) The presence of an intrinsic axial stress σ_0, always associated with the growth process of thin films [8]; The residual stress is usually given by different contributions such as surface reconstruction, interaction between different materials and it also depends on the characteristics of the manufacturing process [9, 10]. The related force is:

$$P_2 = hw\sigma_0(1-\upsilon)$$

We can prove that $P_2 >> P_1$, so $P \approx P_1 \approx$ const. In such a way we solve eq. 4 and we find the analytical expression for K_{eff} as:

$$K_{eff} = \frac{q}{z_C} \tag{5}$$

The result is:

$$k_{eff} = \frac{-2L_c P\gamma^2}{2 + L_c^2\gamma^2 - 2\cosh(L_c\gamma) + 2L_c\gamma\sinh[\gamma(L_c + L_1)] - 2L_c\gamma^2(L_c + L_1) - f(\gamma, L_c, L_1, L_2)} \tag{6}$$

where:

$$f(\gamma, L_c, L_1, L_2) = \frac{\left[2e^{\gamma L1}(e^{L_c\gamma} - 1)(1 + e^{(L_c+L_2)\gamma}) + 2L_c\gamma(1 + e^{L\gamma})\right](\cosh(\gamma(L_c + L_1)) - 1)}{(e^{\gamma L} - 1)} \tag{7}$$

and

$$\gamma = \sqrt{\frac{P}{E'I}} \tag{8}$$

If we insert the equation (6) in the equation (2) (where A is the area of only one pad-beam overlap) we can obtain a right expression for the pull-in voltage.
The parameter P is so far unknown but it can be estimated from a good fitting between the theoretical and the experimental values. In figure 6 the pull-in and hold-down voltages are shown for six structures obtained by this procedure, with σ_0=82 MPa: the agreement with the experimental values is good.

St.	V_{pi}^{exp} $[V]$	V_{hd}^{exp} $[V]$	V_{pi}^{theo} $[V]$	V_{hd}^{theo} $[V]$	L_1 $[\mu m]$	L_2 $[\mu m]$	L_c $[\mu m]$	g_0 $[\mu m]$
1	29 ± 3	26 ± 3	30	26	55	120	180	$0,94 \pm 0,05$
2	33 ± 3	28 ± 3	32	29	55	120	180	$1,12 \pm 0,05$
3	30 ± 3	26 ± 3	32	28	55	230	180	$1,05 \pm 0,05$
4	32 ± 3	28 ± 3	35	28	55	120	180	$1,03 \pm 0,05$
5	42 ± 3	35 ± 3	36	30	55	120	180	$1,18 \pm 0,05$
6	43 ± 3	36 ± 3	46	38	22	120	165	$1,20 \pm 0,05$

Fig. 6. Pull-in and hold-down voltage values experimental and theoretical, fitted with σ_0=82MPa, for six different structures.

DYNAMIC RESPONSE

The switches have been tested with a pulsed actuation voltage too. In such a way we measured the variations of actuation (t1) and de-actuation (t2) times for different applied voltages and for different pulse frequencies. As we can see in figure 7 the pulse frequency doesn't affect the actuation and de-actuation times, while there is a strong influence on the applied voltage (the figure shows the data from a switch with V_{PI}=29V). Time t1 ranges from 500-600μs, with $V=V_{PI}$, to 20-30μs, with $V=2V_{PI}$. Time t2 has been found to be constant in the range 120-130μs for $V>1,1V_{PI}$. The initial increase of t2 can be related to a different deformation of the bridge when it touches the substrate due to different applied voltages.

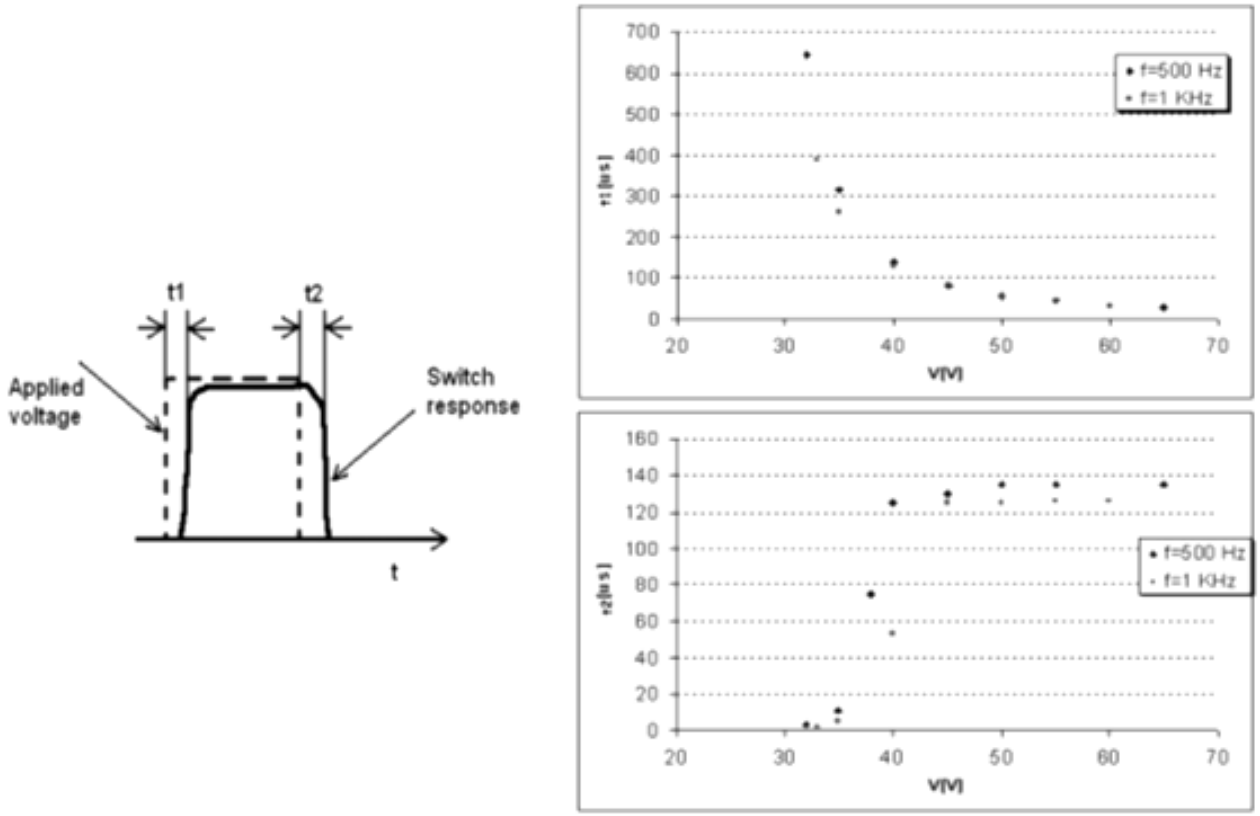

Fig. 7. Left: actuation and de-actuation times definition.
Right: times t1 and t2 versus applied voltages.

CONCLUSIONS

A MEMS switch manufacturing process has been shown, together with its analytical characterization. The building of the devices has been obtained with photolithography techniques by optimization of the materials and parameters.
The electrostatic switches show a pull-in voltage in the range of 29-43 V; their actuation times show a dependence on the applied voltage (in agreement with the theory), while the release times are approximately constant.
The analytical expressions for the pull-in and hold-down voltages have been exploited to find the real air gap bridge-substrate: a substantial reduction, from its nominal value, is present. It is supposed that this deformation is related to the wet etching process of sacrificial layer or to the mechanical properties of the bridge.
An analytical expression for the constant stiffness K_{eff} related to 1D model has been found and by means of this expression the axial stress σ_0 of the gold film has been evaluated.

REFERENCES

[1] G. M. Rebeiz, "RF-MEMS theory, design and technology", *Wiley-Interscience, (2003).*
[2] S. Pamidighantam, R. Puers, K. Baert, H.A C Tilmans, "Pull-in voltage analysis of electrostatically actuated beam structures with fixed-fixed and fixed-free end condition", *Journal of micromechanics and microengineering*, **12,** 458-464, (2002).
[3] P.M. Osberg, S.D. Senturia, "M-TEST: a test chip for MEMS material property measurement using electrostatically actuated test structures", *Journal of Microelectromechanical systems,* **6,** No.2, 107-117, (1997).
[4] H.B. Palmer, "Capacitance of a parallel-plate capacitor by the Schwartz-Christoffel transformation", *Trans. AIEE*, **56,** 363, (1927).
[5] Landau, Lifshitz, "Theory of elasticity"
[6] S.H. Crandall, N.C. Dahl, T.J. Lardner, "An introduction to the mechanics of solids", *McGraw-Hill.*

[7] S. Timoshenko, “Theory of plates and shells”, *McGraw-Hill,* (1987).
[8] S. Qin, H. Wang, “Residual stresses in micro-structures fabricated by the IC-compatible sacrificial layer technique”, *Mechatronics,* **8,** 427-440, (1998).
[9] H. Luth, “Solid surfaces, interfaces and thin films”, *Springer*
[10] Yin Zhang, Quan Ren, Ya-pu Zhao, “Modelling analysis of surface stress on a rectangular cantilever beam”, *Journal of physics: Applied Physics,* **37**, 2140-2145, (2004).
[11] Petersen, K.E., “Micromechanical switches on silicon”, *IBM J, Res. Develop.,* **23,** 376-385, (1979).